

# Immune-orthogonal orthologues of AAV capsids and of Cas9 circumvent the immune response to the administration of gene therapy

Ana M. Moreno<sup>1,6</sup>, Nathan Palmer<sup>2,6</sup>, Fernando Alemán<sup>3</sup>, Genghao Chen<sup>1</sup>, Andrew Pla<sup>1</sup>, Ning Jiang<sup>4</sup>, Wei Leong Chew<sup>5</sup>, Mansun Law<sup>3</sup> and Prashant Mali<sup>1\*</sup>

**Protein-based therapeutics can activate the adaptive immune system, leading to the production of neutralizing antibodies and the clearance of the treated cells mediated by cytotoxic T cells. Here, we show that the sequential use of immune-orthogonal orthologues of CRISPR-associated protein 9 (Cas9) and adeno-associated viruses (AAVs) evades adaptive immune responses and enables effective gene editing using repeated dosing. We compared total sequence similarities and predicted binding strengths to class-I and class-II major histocompatibility complex (MHC) proteins for 284 DNA-targeting and 84 RNA-targeting CRISPR effectors and 167 AAV VP1-capsid-protein orthologues. We predict the absence of cross-reactive immune responses for 79% of the DNA-targeting Cas orthologues—which we validated for three Cas9 orthologues in mice—yet we anticipate broad immune cross-reactivity among the AAV serotypes. We also show that efficacious *in vivo* gene editing is uncompromised when using multiple dosing with orthologues of AAVs and Cas9 in mice that were previously immunized against the AAV vector and the Cas9 cargo. Multiple dosing with protein orthologues may allow for sequential regimens of protein therapeutics that circumvent pre-existing immunity or induced immunity.**

Protein therapeutics, including protein-based gene therapy, have several advantages over small-molecule drugs. They generally serve complex specific functions and have minimal off-target interference on normal biological processes. However, one of the fundamental challenges to any protein-based therapeutic is the interaction between the therapy and the adaptive immune system. Neutralization of the treatment by circulating antibodies that are released by B cells after activation and clearance of treated cells by CD8<sup>+</sup> cytotoxic T lymphocytes (CTLs) creates a substantial barrier to effective protein therapies<sup>1–4</sup>. Although the delay in the adaptive immune response to novel proteins may allow sufficient time for the initial dose to work for some applications, subsequent doses face faster and stronger secondary immune responses owing to the presence of memory T cells and B cells. Gene transfer studies have also shown that immune responses of the host against the delivery vector and/or therapeutic transgene can eliminate treated cells, therefore limiting the efficacy of the treatment<sup>5–11</sup>.

A common approach to circumventing these issues has been to use human proteins or to humanize proteins by the substitution of non-human components<sup>12,13</sup>. However, this approach is limited to a small set of therapeutic proteins that naturally occur in humans or closely related species. Furthermore, although the humanization of proteins can result in a product that is substantially less immunogenic, they still carry an immunological risk<sup>13</sup>. Another way to circumvent an immune response to protein therapeutics is the removal of immunogenic T cell epitopes<sup>14–16</sup>. Once these epitopes are identified, substitution of key amino acids may reduce the immunogenicity of the protein because modification of critical anchor residues can abrogate binding to MHC molecules and prevent antigen

presentation. However, this can prove difficult owing to the high level of diversity at the human leukocyte antigen (HLA) loci. As epitope engineering must account for the substrate specificity of each different HLA allele, therapeutics would probably require unique modifications for each patient. Although epitope deletion and/or mutation has been successfully applied to several proteins<sup>16,17</sup>, this can only preserve protein function when limited to small numbers of HLA alleles that are not representative of the full diversity of the HLA. Structural modifications, such as PEGylation, have also been known to reduce immunogenicity by interfering with antigen-processing mechanisms. However, there is evidence that polyethylene glycol (PEG)-specific antibodies are elicited in patients who are treated with PEGylated therapeutic enzymes<sup>18–21</sup>.

Furthermore, protein therapies often require repeated treatments due to degradation of the protein, turnover of treated cells or—in the case of gene therapy—reduced expression of the transgene<sup>22,23</sup>. This provides an even greater challenge because repeated exposure to the same antigen can elicit a more robust secondary immune response<sup>24</sup>, which may completely inhibit subsequent dosage or even sensitize the immune system to antigens that remain from the initial exposure. To facilitate efficacious repeat protein therapies, we propose the use of orthologous proteins of which the function is constrained by natural selection, but the structure of which is subject to diversification by forces such as genetic drift. An orthologue, given sufficient sequence divergence, will not cross-react with the immune response generated by exposure to the other orthologues, allowing subsequent doses to avoid neutralization by existing antibodies and treated cells to avoid clearance by activated CTLs.

<sup>1</sup>Department of Bioengineering, University of California San Diego, San Diego, CA, USA. <sup>2</sup>Division of Biological Sciences, University of California San Diego, San Diego, CA, USA. <sup>3</sup>Department of Immunology and Microbiology, The Scripps Research Institute, La Jolla, CA, USA. <sup>4</sup>Department of Biomedical Engineering, The University of Texas at Austin, Austin, TX, USA. <sup>5</sup>Synthetic Biology, Genome Institute of Singapore, Singapore, Singapore. <sup>6</sup>These authors contributed equally: Ana M. Moreno, Nathan Palmer. \*e-mail: [pmali@ucsd.edu](mailto:pmali@ucsd.edu)

As a case study for exploring this approach, we focused on the clustered regularly interspaced short palindromic repeats (CRISPR)–Cas9 system, which is perhaps the most anticipated therapeutic for gene editing<sup>25–35</sup>. Comparative genomics has demonstrated that Cas9 proteins are widely distributed across bacterial species and have diversified through an extensive evolutionary history<sup>36–40</sup>. Although there may be pre-existing immunity to Cas9 proteins from pathogenic or commensal species<sup>41–43</sup>, we hypothesized that this diversity could provide a mechanism to circumvent the induction of immunological memory by using orthologous Cas9 proteins for each treatment.

An additional important consideration is the immunogenicity of the delivery vehicle or administration route for the Cas9 and associated guide RNA (gRNA). In this regard, AAVs have emerged as a highly preferred vehicle for gene delivery because they are associated with low immunogenicity and toxicity<sup>8,9</sup>, which promotes transgene expression<sup>44,45</sup> and treatment efficacy. Despite the relatively low immunogenicity of AAV vectors, antibodies against both the capsid and transgene may still be elicited<sup>10,46–52</sup>. Moreover, the prevalence of neutralizing antibodies against AAVs in the human population<sup>53</sup> and cross-reactivity between serotypes<sup>54</sup> remains a hurdle for efficacious AAV therapy. Although AAVs were initially considered to be non-immunogenic owing to their poor transduction of antigen-presenting cells (APCs)<sup>55</sup>, it is now known that they can transduce dendritic cells<sup>56</sup> and trigger innate immune responses through Toll-like receptor (TLR) signalling pathways<sup>57</sup>. The ability to transduce dendritic cells is dependent on the serotype and genome of the AAVs and may be predictive of overall immunogenicity<sup>58</sup>. A previous study exploring the utility of the AAV–Cas9 system observed a humoral immune response to both AAV and Cas9, as well as an expansion of myeloid and T cells in response to Cas9<sup>52</sup>, highlighting the need to confront this issue while further developing gene therapies.

To evaluate the immune orthogonality of AAV-delivered CRISPR–Cas systems, we analysed 284 DNA-targeting and 84 RNA-targeting CRISPR effectors and 167 AAV VP1 orthologues. By comparing the total sequence similarity of these peptides and their predicted binding strengths to class I and class II MHC molecules, we constructed graphs of immune cross-reactivity and computed cliques of proteins that are orthogonal in immunogenicity profiles. Although MHC epitopes do not predict antibody epitopes, the induction of the more powerful memory response is primarily dependent on reactivation of memory B cells with help from memory T cells through the presentation of antigens on class II MHC molecules<sup>59,60</sup>. We then experimentally confirmed our immunological predictions by assaying treated mice for induction of protein-targeting antibodies and cytotoxicity mediated by T cells against AAV and Cas9 proteins. Finally, we demonstrated—in multiple contexts—that consecutive dosing with immune-orthogonal orthologues circumvents the inhibition of effective gene editing caused by immune recognition of the AAV vector and Cas9.

## Results

**Immune response to AAV and Cas9.** One of the major obstacles for treatment using sequential gene therapy is the presence of neutralizing antibodies against the delivery vehicle and the transgene cargo that are induced by the first administration of the therapy (Fig. 1a). To determine the humoral immune response kinetics to AAV–CRISPR therapeutics (Fig. 1b)—focusing as an exemplar on the AAV8 capsid and the *Cas9* transgene—we initially injected C57BL/6J mice retro-orbitally with  $1 \times 10^{12}$  viral genomes (VG) of AAV8 carrying the *Staphylococcus aureus Cas9* (*SaCas9*) transgene, targeting proprotein convertase subtilisin/kexin type 9 (PCSK9), which is a promising gene target that when disrupted can reduce low-density lipoprotein levels and protect against cardiovascular disease. Consistent with a previous study<sup>61</sup>, mice showed reduced

PCSK9 serum levels as early as one week after injection due to successful *SaCas9*-mediated gene editing, which was sustained for the entire duration of the experiment (four weeks; Fig. 1c). We noted that a subset of the mice developed IgG1 antibodies against the *SaCas9* protein (Fig. 1d). Additionally, mice developed humoral immunity to the AAV8 capsid within one week after injection (Fig. 1e). Finally, we also confirmed a response of CD4<sup>+</sup> T cells against AAV8 and *SaCas9* for a subset of the predicted MHCII epitopes on these proteins using an enzyme-linked immunospot (ELISPOT) analysis (Supplementary Fig. 1). To evaluate the feasibility of multiple dosing with AAV–Cas9, we next investigated whether immune-orthogonal sets of AAV and Cas9 orthologues exist.

**Identifying immune-orthogonal proteins.** Natural selection produces diverse structural variants with conserved function in the form of orthologous genes. We assayed the relevance of this diversity for immunological cross-reactivity of 284 DNA-targeting and 84-RNA targeting CRISPR effectors (Supplementary Table. 1) and 167 AAV orthologues (Supplementary Table 2) by first comparing the overall amino acid sequence similarities of these CRISPR effectors and AAV orthologues, and second, using a more specific constraint of comparing how their respective amino acid sequences are predicted to bind MHC class I and II molecules (Fig. 1f). From these analyses we first obtained an estimate of the comprehensive immune overlap among Cas and AAV orthologues on the basis of the sequence level and, second, a more stringent estimate of the predicted immune overlap on the basis of predicted MHC binding (Fig. 1g,h, Supplementary Fig. 2). Using sequence-level clustering and clique finding methods, we defined many sets of Cas9 orthologues that contained up to 9 members with no 6-mer overlap (Supplementary Fig. 3). Notably, on the basis of MHC-binding predictions, we found—among the set of DNA-targeting Cas proteins (240 Cas9 and 44 Cpf1 proteins)—that 79% of pairs are predicted to have non-cross-reacting immune responses, that is, they are predicted to be orthogonal in immune space (Fig. 1g). By contrast, among AAV capsid (VP1 protein) orthologues, we did not find full orthogonality up to the 14-mer level, even when restricting predictions with MHC-binding strengths (Fig. 1h); this probably reflects the strong sequence conservation and shorter evolutionary history of AAVs<sup>62</sup>. This analysis suggests—consistent with previous observations<sup>63,64</sup>—that exposure to one AAV serotype can induce broad immunity to all AAVs, which presents a considerable challenge to AAV delivery methods because some serotypes are prevalent in human populations. Despite the most divergent AAV serotype (AAV5) showing the least shared immunogenic peptides, there remain tracts of sequences that are fully conserved within the VP1 orthologues. As expected, predicted immune cross-reaction negatively correlates with phylogenetic distance (Supplementary Fig. 4), although there is a substantial variation that was not captured by that regression, suggesting that MHC-binding predictions can refine the choice of sequential orthologues beyond phylogenetic distance alone.

**Confirming humoral immune orthogonality among Cas9 proteins.** To test our immunological predictions and to establish the utility of this approach, we focused on a five-member clique containing the ubiquitously used *Streptococcus pyogenes* Cas9 (*SpCas9*) in addition to the well-characterized *S. aureus* Cas9 (Supplementary Fig. 3). To determine whether either of these proteins have cross-reacting antibody responses, we injected mice with  $1 \times 10^{12}$  VG of either AAV8 or AAVDJ capsids containing *SaCas9* or *SpCas9* transgenes by retro-orbital injections and collected serum at day 0 (before injection) and periodically over 4–6 weeks (Fig. 2a). *SpCas9*-specific antibodies were detected in the plasma of all mice injected with *SpCas9* ( $n=6$ ) but, notably, *SpCas9*-specific antibodies were not detected in mice injected with *SaCas9* ( $n=12$ ; Fig. 2b). Half of

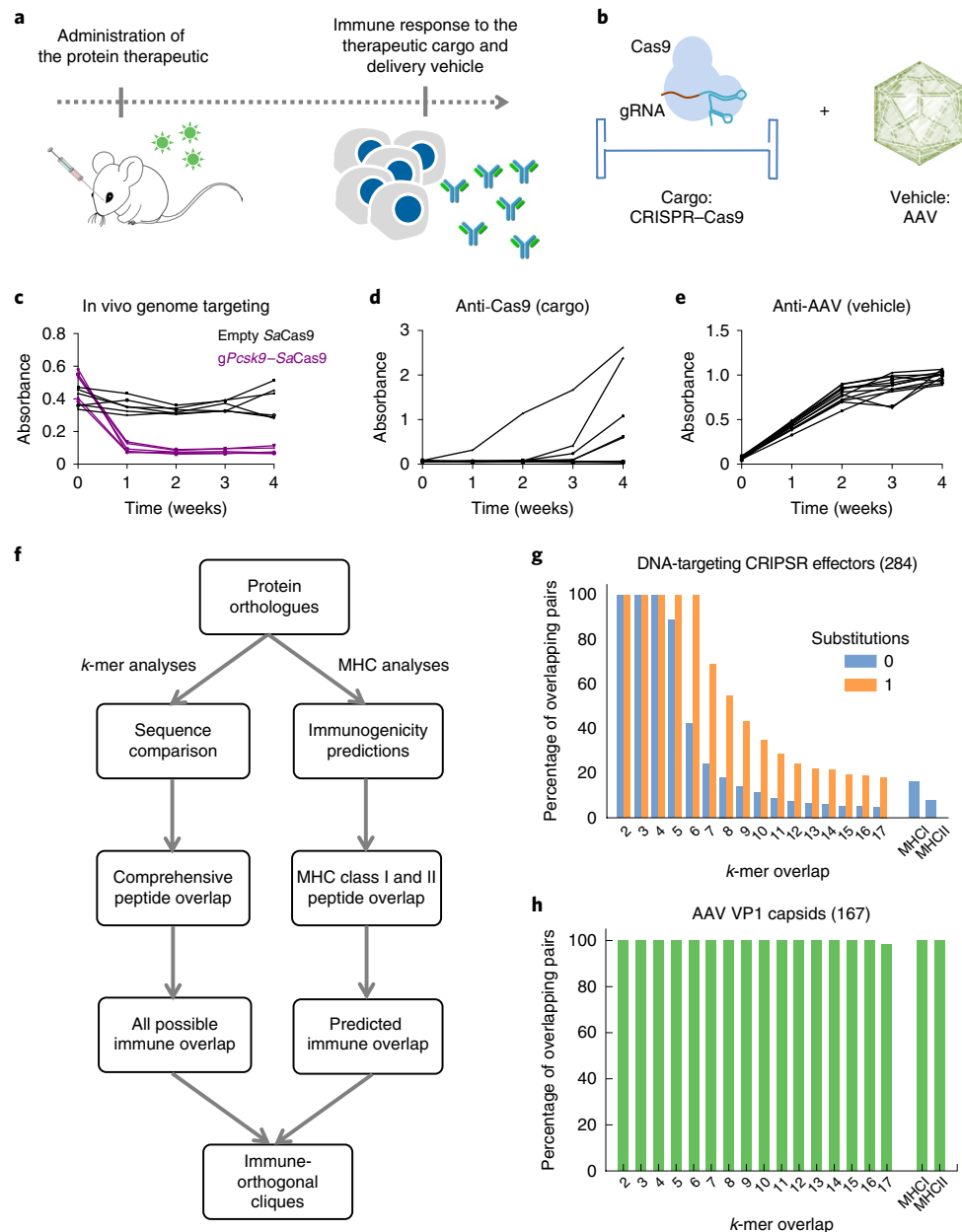


**Fig. 1 | Protein-based therapeutics elicit an adaptive immune response: experimental and in silico analyses.** **a**, Proteins have substantial therapeutic potential, but a major drawback is the immune response to both the therapeutic protein and its delivery vehicle. **b**, As a case study, we studied the CRISPR-Cas9 systems and corresponding delivery vehicles based on AAVs. **c**, Mice were injected retro-orbitally with  $1 \times 10^{12}$  VG per mouse of AAV8-SaCas9 targeting the *Pcsk9* gene or a non-targeting control (empty vector). A decrease in PCSK9 serum levels—owing to successful gene targeting—was observed in mice that received the *Pcsk9*-targeting AAV-SaCas9 virus ( $n=6$  mice for each group). Each line represents an individual mouse. **d**, Immune responses of mice treated with AAV8-SaCas9 to the cargo (Cas9) were detected using ELISAs for the SaCas9 protein ( $n=12$  mice). Each line represents an individual mouse. **e**, Immune responses of mice treated with AAV8-SaCas9 to the delivery vehicle (AAV) were detected using ELISAs for the AAV8 virus capsid ( $n=12$  mice). Each line represents an individual mouse. **f**, The in silico workflow used to find immune-orthogonal protein-homologue cliques. **g**, Immunologically uninformed sequence comparison was carried out by checking all  $k$ -mers in a protein for their presence in another protein sequence with either zero or one mismatch. The  $x$  axis corresponds to  $k$ , whereas MHC I and MHC II show overlap only of peptides predicted to bind to MHC class I and class II molecules; 48% of Cas9 pairs show no 6-mer overlap, and 79% of pairs show no overlapping MHC-binding peptides. **h**, Immunologically uninformed sequence comparison as in **g** but for AAV VP1 capsid proteins. All AAV pairs contain overlapping MHC-binding peptides.

the mice injected with AAVs carrying the SaCas9 transgene ( $n=12$ ) developed detectable antibodies against SaCas9, whereas none of the mice injected with AAVs carrying the SpCas9 transgene ( $n=6$ ) developed an antibody response against SaCas9. These results were confirmed in an independent study in which SpCas9-specific antibodies—but not SaCas9-specific antibodies—were detected in the

plasma of mice injected with AAV-SpCas9 ( $n=12$ ). These mice were injected retro-orbitally with  $1 \times 10^{12}$  VG of AAV8-SpCas9 or AAVDJ-SpCas9 and also received an additional intramuscular injection of  $1 \times 10^{11}$  VG at week 4 (Fig. 2c). Taken together, our data confirms that SpCas9 and SaCas9 have humoral immune orthogonality. As an additional step, we tested another Cas9 orthologue

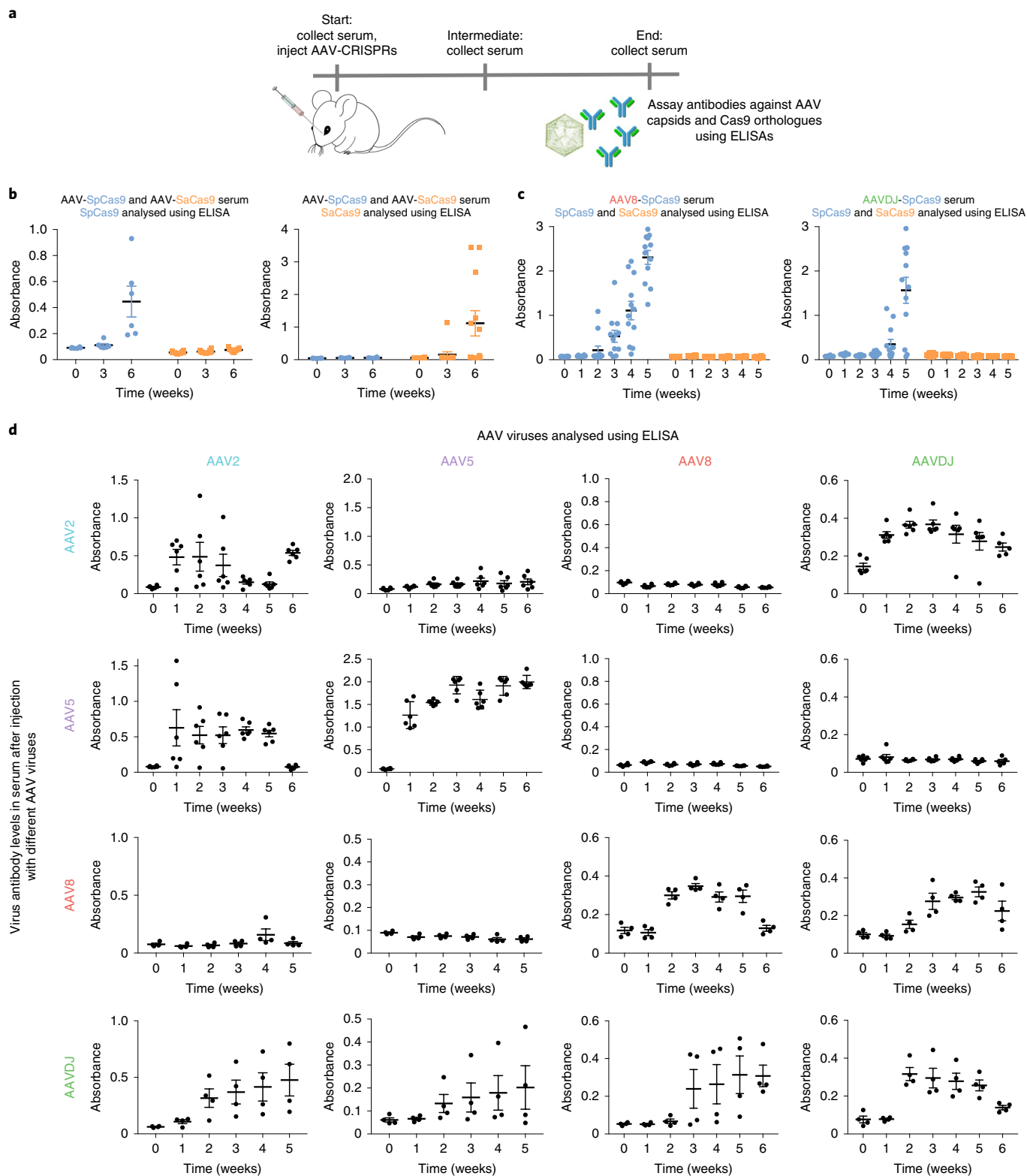


**Fig. 2 | Experimental validation of Cas9 and AAV immunogenicity predictions.** **a**, Mice were exposed to antigens by retro-orbital injections at  $1 \times 10^{12}$  VG per mouse. Serum was collected before injection on day 0, and at multiple points over the course of 4–6 weeks. **b**, Levels of anti-SpCas9 antibodies generated in mice injected with either SpCas9 ( $n=6$ ) or SaCas9 ( $n=12$ ), and levels of anti-SaCas9 antibodies generated in mice injected with either SpCas9 ( $n=6$ ) or SaCas9 ( $n=12$ ). Data are mean  $\pm$  s.e.m. Each data point represents an individual mouse. **c**, Levels of anti-SpCas9 and anti-SaCas9 antibodies generated by mice injected retro-orbitally  $1 \times 10^{12}$  VG on day 0 and intramuscularly with  $1 \times 10^{11}$  VG on week 4 with AAV8-SpCas9 ( $n=12$ ; left) or AAVDJ-SpCas9 ( $n=12$ ; right). Data are mean  $\pm$  s.e.m. Each data point represents an individual mouse. **d**, Levels of anti-AAV8/AAVDJ/AAV2/AAV5 antibodies generated in mice injected with either AAV8 or AAVDJ ( $n=4$  for all panels), or with either AAV2 or AAV5 ( $n=6$  for all panels except for the AAVDJ serum ELISA at the week 6 time point for which  $n=5$ ). Data are mean  $\pm$  s.e.m. Each data point represents an individual mouse.

from *Campylobacter jejuni*, which is useful for AAV-based delivery owing to its small size. Mice injected retro-orbitally with  $1 \times 10^{12}$  VG AAV8-CjCas9 ( $n = 12$ ) showed no significant humoral response to SpCas9 or SaCas9 after 4 weeks (Supplementary Fig. 5), confirming immune orthogonality for a set of three unique Cas9 orthologues.

**Confirming broad immune cross-reactivity among AAV serotypes.** AAVs are becoming a preferred delivery vehicle owing to their ability to avoid the induction of a strong CD8<sup>+</sup> T cell response; however, the presence of neutralizing antibodies remains a substantial barrier to successful application of AAV therapies. Consistent with previous results<sup>63</sup>, we found shared immunogenic peptides among all human AAV serotypes (Supplementary Fig. 6). We confirmed the lack of orthogonality for two serotypes—AAV8 and AAVDJ—in which we found that antibodies produced in mice injected with AAV8 or AAVDJ react to both AAV8 and AAVDJ antigens (Fig. 2d). Our analysis suggests that there are no two known AAVs for which exposure to one would guarantee immune naivety to another across all MHC genotypes. However, immune cross-reaction could be minimized through the use of AAV5<sup>64,65</sup>, the most phylogenetically divergent serotype. Our predictions identify only one highly immunogenic peptide that is shared between AAV5 and the commonly used AAV2 and AAV8 in the mouse model (although several other shared peptides with mild MHC affinity exist). We confirmed this by analysis using enzyme-linked immunosorbent assays (ELISAs), in which mice injected with AAV2 did not elicit antibodies against AAV5 and AAV8, and mice injected with AAV5 did not elicit antibodies against AAVDJ and AAV8 (Fig. 2d).

**Overcoming immune barriers to effective gene editing.** Having demonstrated that AAV-Cas9 viruses elicit an immune response in the mouse model and that the humoral responses to SpCas9 and SaCas9 do not cross-react, we then performed a two-step dosing experiment to test whether these immune responses inhibit the efficacy of multi-dose gene editing, and whether using immune-orthogonal orthologues in sequence can avoid immune-mediated inhibition of gene editing (Fig. 3a, Supplementary Fig. 7). For this experiment we used BALB/c mice to verify and characterize the immune response in two independent strains. The first round of dosing contained no gRNA and served to immunize the mice against the second dose, which contained an active AAV8-SaCas9 containing a *Pcsk9*-targeting gRNA, allowing us to directly measure genome editing efficiency by sequencing, as well as measure the levels of serum PCSK9 as a phenotypic readout for therapeutic efficacy. We also measured IgG responses to all AAV and Cas9 used in the experiment. As expected from previous preclinical studies on AAV therapies, previous exposure and humoral immunity to AAV8 (AAV8-mCherry) abolished the effectiveness of

subsequent gene editing when using AAV8 as the delivery vector (AAV8-SaCas9). Importantly, this effect was not seen with previous exposure to AAV5 (AAV5-mCherry), and subsequent dosing with AAV8-SaCas9 resulted in strong genome editing and *Pcsk9* knockdown similar to the effects of AAV8-SaCas9 treatment in naive mice (Fig. 3b,c).

Although we do not necessarily expect the orthogonality that was observed between AAV8 and AAV5 to carry over into the human setting, here it allowed us to specifically test the effects of the immune response to the *cas9* cargo with minimal interference from the AAV delivery vector. Mice that were first immunized against SaCas9 using AAV5 showed a 35% reduction in the level of editing, a 38% reduction in the decrease in serum levels of PCSK9 and a wider variation between mice compared with the unimmunized (saline-treated) mice. This may reflect a weak immune response to SaCas9 in our mouse model and/or a domination of private (individual) T cell responses to SaCas9. IgG ELISAs revealed that only a subset of mice immunized with AAV5-SaCas9 developed an antibody response. We correlated the level of serum antibodies induced on SaCas9 immunization with the efficiency of *Pcsk9* editing after the second dose, and we found that mice with a stronger antibody response showed lower editing efficiency (Supplementary Fig. 7b). By contrast, we found that mice first dosed with AAV5-SpCas9 showed robust editing similar to that in naive mice, suggesting that the predicted and measured immune orthogonality of SpCas9 and SaCas9 can be harnessed to circumvent immune barriers to gene editing.

To replicate these findings in a different context, and to verify that immunity to Cas9 can specifically create a barrier to effective gene therapy, we conducted a slightly modified immunization experiment. We used a Cas9 protein vaccine combined with complete Freund's adjuvant (CFA) in emulsion as the initial dose, thereby immunizing a Cas9-specific primary response independently of AAV (Fig. 3d). Subsequent dosing with AAV8-SaCas9 targeting PCSK9 recapitulated the results of AAV-based immunization, showing that previous exposure to the SaCas9 protein—but not SpCas9—significantly reduced the effectiveness of SaCas9-based gene editing (Fig. 3e,f). We also tested the ability of CFA-Cas9 immunized mice to clear injected splenocytes pulsed with immunogenic Cas9 epitopes. We observed specific clearance of Cas9-pulsed cells 3.5 weeks after immunization, demonstrating that anti-Cas9 T cells can specifically recognize and kill cells that present Cas9 epitopes (Supplementary Fig. 8).

Taken together, anti-AAV and anti-Cas9 immunity represents a potential obstacle to therapeutic efficacy, and the use of immune orthogonal AAVs and Cas proteins—by bypassing immune recall—enables effective gene editing using repeated administrations of these therapeutic modalities.

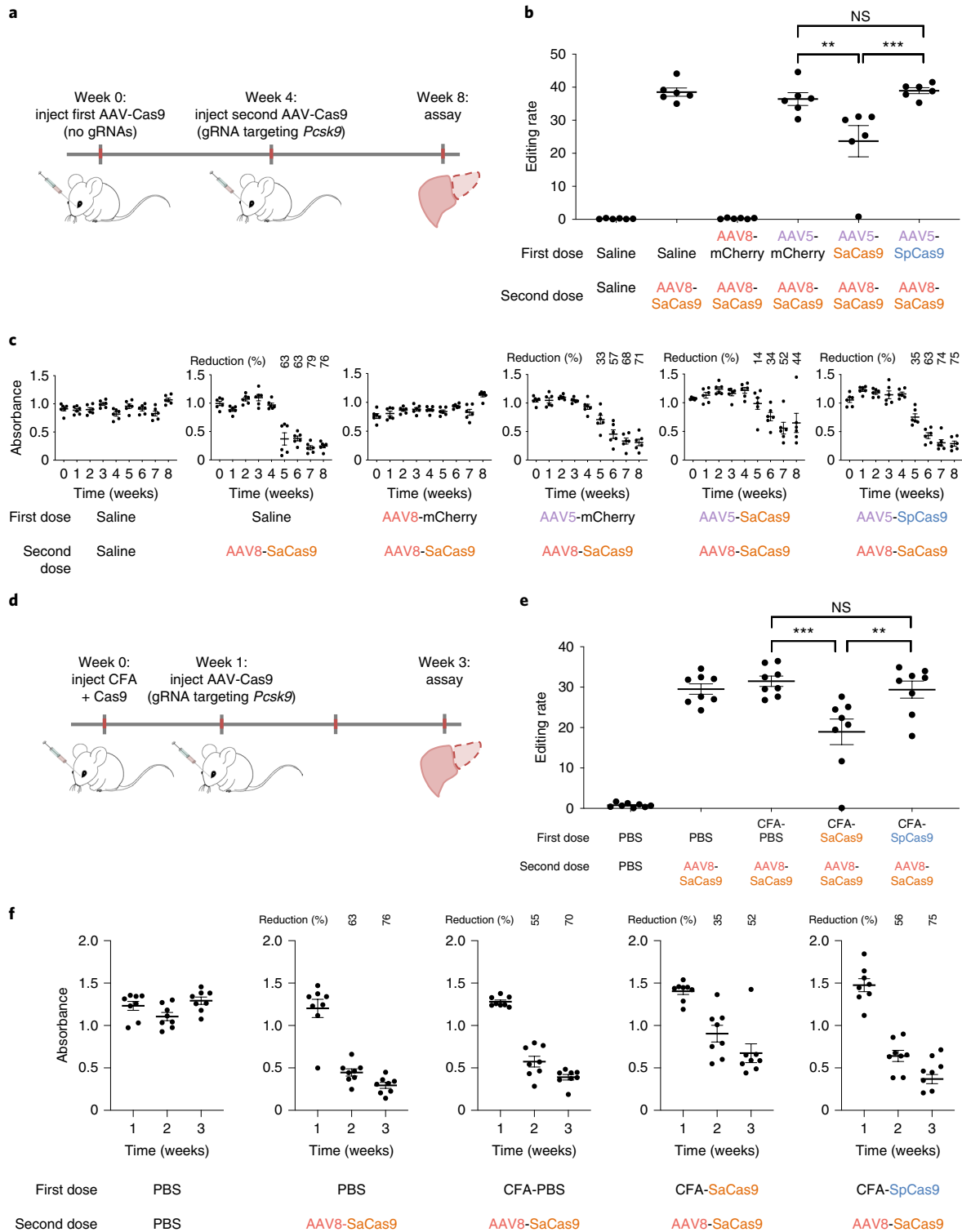
**Fig. 3 | Engineering re-dosing with immune orthogonal orthologues.** **a**, Mice were initially immunized with saline, AAV8-mCherry, AAV5-mCherry, AAV5-SaCas9 or AAV5-SpCas9 with no gRNA. After 4 weeks, the mice were given a second dose of saline or AAV8-SaCas9 with a gRNA targeting *Pcsk9*. Serum was collected before the first injection and again during each subsequent week for 8 weeks. Mice were exposed to antigens by retro-orbital injections at  $1 \times 10^{12}$  VG per mouse. **b**, Genome editing rates—quantified by sequencing—are entirely abolished when mice are immunized against AAV8 and moderately inhibited when immunized against SaCas9. No effect is seen when mice are immunized against AAV5 or SpCas9. Data are mean  $\pm$  s.e.m. A one-way analysis of variance (ANOVA) with post hoc Tukey's test was performed to determine statistical differences.  $^{**}P = 0.0033$ ;  $^{***}P = 0.0004$ ; NS, not significant. Each data point represents an individual mouse ( $n = 6$  for all panels). **c**, Final PCSK9 serum levels (week 8), the phenotypic result of gene editing, decrease sharply after an active second dose of AAV8-SaCas9 with gRNA. This effect is abolished when mice are first immunized against AAV8, but not when mice are first immunized against AAV5. Previous immunization with AAV5-SaCas9 reduces but does not eliminate editing, whereas previous dosing with AAV5-SpCas9 has no effect on editing. Data of the full time-course for each week are shown. Data are mean  $\pm$  s.e.m. Each data point represents an individual mouse ( $n = 6$  for all panels). **d**, Mice were immunized with both CFA and 5  $\mu$ g Cas9 1 week before injections with active AAV-SaCas9. **e**, At week 3, mice immunized with SaCas9 show a reduced editing rate compared with mice injected with both CFA and PBS. No change in editing rate is seen when immunized with SpCas9. Data are mean  $\pm$  s.e.m. A one-way ANOVA with post hoc Dunnett's test was performed to determine statistical differences.  $^{***}P = 0.0002$ ;  $^{**}P = 0.0015$ ; NS, not significant. Each data point represents an individual mouse ( $n = 8$ ). **f**, The reduction in serum PCSK9 is partially inhibited when mice are immunized with both CFA and SaCas9, but not with CFA and PBS, or CFA and SpCas9. Data are mean  $\pm$  s.e.m. Each data point represents an individual mouse ( $n = 8$ ).

Discussion

The use of protein therapeutics requires ways to evade the immune response of the host. Cas9, for example, has prokaryotic origins and can evoke a long-lived T cell response<sup>42,52</sup> that may lead to the clearance of transduced cells. Furthermore, circulating antibodies can neutralize the AAV vector and prevent efficient transduction after repeated doses. Immunosuppressive drugs could mitigate some of these aspects, but not without considerable side effects, and these drugs are not applicable to patients in poor health<sup>66–69</sup>. Similar to

what has been done using cancer-targeting antibody therapeutics<sup>70</sup>, the SpCas9 protein could be deimmunized by swapping high-immunogenicity domains. This is a promising approach; however, it will be complex and laborious as we anticipate tens of mutations to achieve stealth, which might often result in a reduction in activity and a less effective therapy overall.

Another consideration is that various applications of the CRISPR system will have substantially different consequences on the immune system. For example, compare genome-editing applications—in



which only transient expression of Cas9 is required—with cases of gene regulation (CRISPR interference or CRISPR activation), in which continuous Cas9 expression is required. Although ongoing expression applications will have to continuously contend with T cell surveillance, genome editing with transient expression may not be compromised by a primary T cell response if Cas9 expression is lost before CTL activation and clonal expansion. Building on this advantage, we note that promising new techniques may achieve stable gene regulation by transient—that is, hit-and-run—approaches using epigenome editing<sup>71</sup>. Despite this, efficacious single-dose therapies may require high titres, especially in cases such as Duchenne muscular dystrophy, in which systemic delivery is needed. Such high doses may lead to toxicity issues, as demonstrated in a recent study of high-dose AAV9 delivery in rhesus macaques<sup>72</sup>. Multiple lower non-toxic doses delivered sequentially have the potential to achieve high transduction efficiency but must contend with a stronger and faster secondary adaptive immune response that is mediated by memory T cells and B cells.

To circumvent this issue, here we developed a framework to compare protein orthologues and their predicted binding to MHC I and MHC II by checking a sliding window of all *k*-mers in a protein for their presence in another, focusing on peptides that we predicted would bind to at least one MHC allele. Through this analysis, we identified cliques of Cas9 proteins that are immune orthogonal. On the basis of these predictions, specific T cell responses from one orthologue would not cross-react with another orthologue of the same clique, preventing the reactivation of CD8<sup>+</sup> cytotoxic T cells, as well as the CD4<sup>+</sup> helper T cells necessary to reactivate memory B cells. We confirmed these results through ELISAs and verified that three well-characterized Cas9 proteins (*SpCas9*, *SaCas9* and *CjCas9*) are immune orthogonal. Finally, we demonstrated in multiple contexts that consecutive dosing with the same AAV or Cas9 orthologue can lead to diminished editing efficacy that can be overcome with the use of immune orthogonal orthologues. Therefore, we expect that proteins belonging to the same clique can be used sequentially without eliciting responses of memory T cells and B cells.

An important caveat is that each sequential orthologue should also be immune orthogonal to the pre-existing immune repertoire. Recent research has begun to explore pre-existing immunity to *SpCas9* and *SaCas9*<sup>41–43</sup> in human donors. One potential repository of Cas9 to which humans may not have any pre-existing immunity is in the genomes of extremophiles. However, although humans have probably not been exposed to these organisms previously, their Cas9 proteins may nevertheless be closely related to commensal or pathogenic species, and therefore immune orthogonality to pre-existing immunity must be rigorously evaluated. To explore this issue, we categorized 240 Cas9s orthologues on the basis of their species of origin as commensal, pathogenic, environmental or extremophile, and compared the immune orthogonality between these groups (Supplementary Fig. 9). Preliminary analysis suggests that there may be Cas9 proteins from extremophile species that are divergent enough to be orthogonal to pre-existing immunity, even when taking into account both pathogens and commensals. Many more candidates will probably be discovered as we continue cataloguing microbial diversity in a variety of environments using metagenomic approaches. Alongside this process, more diverse Cas9 proteins must be tested and studied to determine whether—and under what conditions—they will be usable in a mammalian setting.

Owing to the importance of AAVs as a delivery agent in gene therapy, we also analysed AAV serotypes through our MHC I and II comparison framework and have demonstrated that no two AAVs are predicted to be entirely immune orthogonal. However, with a known HLA genotype, it may be possible to define a personalized regimen of immune orthogonal AAVs using serotypes that are already defined. For instance, use of AAV5 minimizes immune

cross-reactivity in mice and non-human primates, as demonstrated by a recent study in which chimaeric-AAV5-immunized mice and non-human primates successfully received a second dose of treatment with AAV1<sup>65</sup>. However, in the human setting, we predict that there may be substantially more immune overlap between AAV5 and other AAVs. It has also been shown that memory B cells heavily contribute to the antibody response to similar but not identical antigens<sup>73</sup>, indicating that partial orthogonality may not be sufficient. Our analysis suggests that creating a pair of globally orthogonal AAV capsids for human application would require more than ten mutations in one of the two proteins. This hypothetical orthogonal AAV capsid presents a substantial engineering challenge, as it requires mutating many of the most conserved regions to achieve immune orthogonality.

Although we characterize the adaptive immune response to both the AAV VP1 and Cas9 proteins, it is not expected that these will induce the same type or kinetics of response due to the differing nature of the antigens. The mice receive VP1 protein in the form of a viral capsid, as contrasted with Cas9 in the form of DNA. The delivery of AAV capsids is expected to produce a strong antibody response through the canonical MHC class II pathway. It may also induce a CTL response through MHC class I presentation by transduction of APCs or cross-presentation of endocytosed viral proteins.

Alternatively, the Cas9 transgene is expressed as protein only once inside a transduced cell, and therefore could be expected to induce both an antibody and CTL response through two separate but not mutually exclusive mechanisms. One potential avenue is that a subset of AAVs transduce APCs, an event that has been previously observed to occur<sup>56</sup>. After expression, Cas9 may be presented on class I MHC molecules through the canonical pathway or presented on class II MHC molecules after being encapsulated in autophagosomes (a substantial fraction of MHCII-bound peptides is derived from internal proteins through autophagy)<sup>74</sup>. Another potential mechanism involves transduced non-APCs expressing Cas9 and subsequently undergoing apoptosis or necrosis. APCs then scavenge these dying cells, presenting the Cas9 proteins found within on class II MHC molecules through the canonical pathway or on class I MHC molecules through cross-presentation—a process that is important for anti-viral immune responses.

Previous research has identified that MHC affinity is highly dependent on anchor residues at both ends of its binding pocket<sup>75</sup>. Residue diversity is more tolerated in the centre of the binding pocket—although these residues may have the greatest effect on antigen specificity—as it is thought that these residues are central to the interaction with the T cell receptor (TCR). A comparison of the number of orthologous pairs in 9-mer space with the number of predicted orthologous pairs on the basis of class-II-binding predictions indicates that only approximately 65% of 9-mer peptides serve as appropriate MHC class II binding cores, even across the thousands of HLA-2 combinations that we explored here. This undersampling of peptide space by MHC molecules probably reflects the requirement for hydrophobic anchor residues in the MHC binding pocket and leaves room for protein deimmunization through mutation of immunogenic peptides to ones that never serve as MHC binding cores. However, achieving these mutations while preserving protein function has proven to be difficult even for small numbers of HLA alleles, and remains a major protein engineering challenge. New technologies for directly measuring TCR affinity with MHC-presented antigens<sup>76</sup> will also further clarify the key antigenic peptides contributing to the immune response, and will be useful to inform approaches here.

We also note some limitations to our study. We mainly used two inbred mouse strains—C57BL/6J and BALB/c—as our model; these strains of mice have limited MHC diversity<sup>77</sup> and might not recapitulate other human immunological features, such as differences in

antigen processing and presentation. Our use of highly conservative models of potential human immunity suggests that any immune barriers to gene editing that we observe here could be substantially magnified in the human setting. We therefore attempted to measure the human T cell response using an IFN $\gamma$  ELISPOT assay for a subset of the predicted MHC I and MHC II peptides (Supplementary Tables 3 and 4), the results of which corroborated recent studies of pre-existing immunity to SpCas9 and SaCas9 in humans<sup>16,41,42</sup> that showed measurable effector and regulatory T cell responses. We observed a low CD4<sup>+</sup> T cell response against specific MHC II peptides for mice injected with SaCas9 in our C57BL/6J model (Supplementary Fig. 1). One promising approach is to harness the ability of regulatory T cells to promote a more tolerogenic immune response to therapeutic proteins<sup>42</sup>. Additionally, B cell epitopes can also be predicted and incorporated into immune orthogonality analysis. However, these are more difficult to predict because B cell epitopes may be both linear and conformational. Advances and further validation of these *in silico* models will enable better predictions in the future<sup>78–82</sup>. In our study, initial immunization doses were not delivered with a gRNA, therefore, Cas9 produced inside the cell or delivered as a protein will be in the apo-Cas9 conformation. This could result in different B cell epitopes compared with the gRNA-bound Cas9 complex, as the three-dimensional conformations are substantially different. Note, however, that this should not affect MHC-presented peptides, and therefore not affect T cell responses. Finally, recent research has indicated that spliced-host and pathogen-derived peptides created by proteasomal processing might make an important contribution to MHC class I peptides<sup>83</sup>. It is unclear how this could affect cross-recognition of the proteins that we predict to be immune orthogonal, but it provides a mechanism by which cross-recognition of substantially different foreign antigens might result from very-short antigenic peptides spliced to the same host protein; however, we think that this is improbable owing to the large number of possible spliced peptides between the antigen and entire host proteome.

Overall, we believe that our framework provides a potential solution for efficacious gene therapy, not only for Cas9-mediated genome engineering, but also for other protein therapeutics that might necessitate repetitive treatments. Although the use of this approach still requires mitigation of the primary immune response—particularly antibody neutralization and CTL clearance—we expect that epitope deletion and low-immunogenicity delivery vectors, such as AAVs, will mitigate this problem, and the potential for repeated dosage will reduce the need for very high first-dose titres and efficiency.

## Methods

**Computational methods.** *k*-mer analyses. For Cas9, we initially chose 91 orthologues that were cited in exploratory studies cataloguing the diversity of the Cas9 protein<sup>36,39,40,84–86</sup>, including several that are experimentally well characterized. We subsequently expanded our analysis to a total of 240 Cas9 orthologues and 44 Cpf1–Cas12a orthologues for DNA-targeting CRISPR-associated effector proteins, and 84 RNA-targeting CRISPR-associated effectors including Cas13a, Cas13b and Cas13c. For AAVs, we analysed 167 sequences, focusing on all 13 characterized human serotypes as well as one isolate from rhesus macaque (rh32), one engineered variant (DJ) and one reconstructed ancestral protein (Anc80L65). We then compared the total sequence similarity (immunologically uninformed) between these peptides as well as comparing their predicted binding to class I and class II MHC molecules (immunologically informed). Immunologically uninformed sequence comparisons were carried out by checking a sliding window of all contiguous *k*-mers in a protein for their presence in another protein sequence with either zero or one mismatch.

**MHC binding predictions.** An immunologically informed comparison was performed in a similar fashion but using only those *k*-mers that were predicted to bind to at least 1 of 81 HLA-I alleles using netMHC v.4.0<sup>87</sup> for class I (alleles can be found at [http://www.cbs.dtu.dk/services/NetMHC/MHC\\_allele\\_names.txt](http://www.cbs.dtu.dk/services/NetMHC/MHC_allele_names.txt)) and at least 1 of 5,620 possible MHC II molecules on the basis of 936 HLA-2 alleles using netMHCIIpan v.3.1<sup>88</sup> for class II (alleles can be found at [http://www.cbs.dtu.dk/services/NetMHCIIpan-3.1/alleles\\_name.list](http://www.cbs.dtu.dk/services/NetMHCIIpan-3.1/alleles_name.list)).

We compared the use of netMHC with alternative immune epitope prediction platforms methods, such as the Immune Epitope Database (<https://www.iedb.org>)<sup>89</sup>, and found very strong agreement across software. Ultimately, we chose netMHC owing to the larger number of HLA alleles it supports. Sequences were defined as binding if the predicted affinity ranked in the top 2% of a test library of 400,000 random peptides, as suggested in the software guidelines. The generation of immune orthogonal cliques was performed using the Bron–Kerbosch algorithm. In brief, a graph was constructed with each orthologue as a vertex, in which the edges are defined by the number of shared immunogenic peptides between the connecting vertices. Sets of proteins in which every pair in the set is immune orthogonal constitute a clique.

**Phylogenetics and species classification.** For phylogenetic analyses, protein sequences were aligned using MUSCLE, and distance was calculated using the BLOSUM 62 matrix excluding insertions and deletions. A phylogeny of AAV serotypes was created using neighbour joining on major serotype sequences. Categorization of Cas9 orthologues into commensal, pathogenic, environmental and extremophile species of origin was performed by assessing the source of the sample sequence. Sequences that were isolated from species that had been observed in human-associated samples were classified as pathogenic if they had been reported to cause disease (this included species that are normally commensal, but opportunistically pathogenic), otherwise, they were reported as commensal. Sequences from species that are not known to be associated with the human microbiome were classified as environmental unless the species was uniquely isolated from extreme environments including geothermal vents, deep anoxic groundwater, fossil fuel deposits and polar ice.

**Experimental methods. Vector design and construction.** Split-SpCas9 AAV vectors were constructed by sequential assembly of corresponding gene blocks (IDT) into a custom synthesized rAAV2 vector backbone<sup>90,91</sup>. The first AAV contains a gRNA driven by a human RNA polymerase III promoter, U6 and a N-terminal Cas9 (NCas9) construct fused to an N-intein driven by a CMV promoter, as well as a polyadenylation (polyA) signal. The second AAV cassette contains a CMV-driven C-terminal Cas9 (CCas9) construct fused to a C-intein as well as a polyA signal. gRNA sequences were inserted into NCas9 plasmids by cloning oligonucleotides (IDT) encoding spacers into AgeI cloning sites using Gibson assembly. pX601-AAV-CMV::NLS-SaCas9-NLS-3xHA-bGHpA;U6::BsaI-sgRNA was a gift from F. Zhang (Addgene plasmid, 61591).

**AAV production.** AAV2/8, AAV2/2, AAV2/5 and AAV2/DJ virus particles were produced by HEK293T cells using the triple transfection method and purified with an iodixanol gradient<sup>92</sup>. Confluency at transfection was between 80% and 90%. Medium was replaced with prewarmed medium 2 h before transfection. Each virus was produced in 5 × 15 cm<sup>2</sup> plates, and each plate was transfected with 7.5  $\mu$ g of pXR-capsid (pXR-8, pXR-2, pXR-5 or pXR-DJ), 7.5  $\mu$ g recombinant transfer vector and 22.5  $\mu$ g of pAd5 helper vector using polyethylenimine (PEI; 1  $\mu$ g  $\mu$ l<sup>-1</sup> linear PEI in 1 × DPBS pH 4.5, using HCl) at a PEI:DNA mass ratio of 4:1. The mixture was incubated for 10 min at room temperature and then applied dropwise onto the medium. The virus was collected after 72 h and purified using an iodixanol-density-gradient ultracentrifugation method. The virus was then dialysed with 1 × PBS (pH 7.2) supplemented with 50 mM NaCl and 0.0001% of Pluronic F68 (Thermo Fisher) using 100 kDa filters (Millipore) to a final volume of around 1 ml, and quantified by qPCR using primers specific to the inverted terminal repeat (ITR) region, against a standard (ATCC VR-1616). The primers used were as follows: AAV-ITR-F, 5'-CGGCCTCAGTGAGCGA-3'; and AAV-ITR-R, 5'-GGAACCCCTAGTGATGGAGTT-3'.

**Animal studies.** All animal procedures were performed in accordance with protocols approved by the Institutional Animal Care and Use Committee (IACUC) of the University of California, San Diego. All mice were acquired from the Jackson Laboratory. AAV injections were performed in adult male C57BL/6J or BALB/c mice (10 weeks old) through retro-orbital injections using 1 × 10<sup>12</sup> VG per mouse.

**CFA immunizations.** CFA immunizations were prepared by mixing CFA (Sigma-Aldrich) with 5  $\mu$ g Cas9 protein or PBS at a 1:1 ratio using two syringes connected by an elbow joint to create an even emulsion. Then, 200  $\mu$ l of CFA emulsion was injected subcutaneously into the flanks of adult mice.

**ELISA.** Levels of serum PCSK9 were measured using the Mouse Proprotein Convertase 9/PCSK9 Quantikine ELISA kit (R&D Systems) according to the manufacturer's guidelines. In brief, serum samples were diluted 1:200 in Calibrator diluent and allowed to bind for 2 h onto microplate wells that were precoated with the capture antibody. Samples were then sequentially incubated with PCSK9 conjugate followed by the PCSK9 substrate solution with extensive intermittent washes between each step. The amount of PCSK9 in serum was estimated colorimetrically using a standard microplate reader (BioRad iMark).

ELISA for Cas9 and AAV was performed as follows. Recombinant SpCas9 protein (PNA Bio, CP01), or SaCas9 protein (ABMgood, K144), was diluted in 1 × coating buffer (Bethyl), and 0.5  $\mu$ g was used to coat each well of 96-well Nunc

MaxiSorp plates (ab210903) overnight at 4°C. For AAV experiments,  $1 \times 10^9$  VG of AAV2, AAV5, AAV8 or AAVDJ in  $1 \times$  coating buffer was used to coat each well of 96-well Nuc MaxiSorp plates. Plates were washed three times for 5 min with 350  $\mu$ l of  $1 \times$  wash buffer (Bethyl) and blocked with 300  $\mu$ l of  $1 \times$  BSA blocking solution (Bethyl) for 2 h at room temperature. The wash procedure was repeated. Serum samples were added at 1:40 dilution and plates were incubated for 5 h at 4°C with shaking. Wells were washed three times for 5 min and 100  $\mu$ l of HRP-labelled goat anti-mouse IgG1 (Bethyl; diluted 1:100,000 in  $1 \times$  BSA blocking solution) was added to each well. After incubating for 1 h at room temperature, wells were washed four times for 5 min, and 100  $\mu$ l of TMB substrate (Bethyl) was added to each well. Optical density at 450 nm ( $OD_{450}$ ) was measured using a plate reader (BioRad iMark).

**NGS quantification of editing.** Genomic DNA was extracted from samples of mouse livers using a DNA extraction kit (Qiagen). A 200 bp region containing the target cut site of the *Pcsk9* gene was amplified by PCR using 0.5  $\mu$ g DNA (around 100,000 diploid genomes) as the template. Libraries were prepared using NEBNext Illumina library preparation kit and sequenced using an Illumina HiSeq. Each sample was sequenced to a target depth of 100,000 reads. Adaptors were trimmed from resulting fastqs using AdapterRemoval<sup>93</sup> and non-homologous end-joining-repaired cleavage events resulting in a mutation were quantified using CRISPResso<sup>94</sup>.

**Splenocyte clearance assay.** Splenocyte clearance assays were performed similarly to previous research<sup>95</sup>. In brief, spleens from adult C57BL/6J mice were collected and treated to remove erythrocytes and dead cells. These cells were then diluted to  $1 \times 10^7$  cells  $ml^{-1}$  and split into two pools, one of which was pulsed for 40 min with a pool of the 30 most immunogenic T cell epitopes in SpCas9 (according to our predictions) at 1  $\mu$ g  $ml^{-1}$  each and labelled with the CellTrace Violet fluorescent dye (ThermoFisher). The other pool was pulsed with a matching volume of DMSO, and labelled with the green fluorescent dye CFSE (ThermoFisher). A 1:1 mixture of these cells were then retro-orbitally injected into naive or CFA-immunized mice at week 1 or week 3.5 at  $3\text{--}6 \times 10^7$  cells per mouse. Spleens from these mice were collected 16–20 h later, treated to remove erythrocytes and analysed by flow cytometry to assess the degree of specific clearance of the CTV<sup>+</sup> cells that were pulsed with Cas9 peptides.

**Statistics.** PCSK9 ELISA data from immunization experiments (Fig. 3, Supplementary Fig. 7) were normalized per mouse to the average of the first 4 weeks of the experiment (during which time no active dose was given), and then these data were analysed using a two-way repeated-measures ANOVA to account for both time and group membership as independent variables. Post hoc Tukey's tests were used to compare across groups at each time point as shown in Fig. 3c.

**Epitope prediction and peptide synthesis.** The MHC-binding peptides for our mouse model were predicted using the netMHC v.4.0 and netMHCIIpan v.3.1 online software with the alleles H-2-Db and H-2-Kb for class I and H-2-IAb for class II. For MHCII, the top 10 peptides by percentile binding for SpCas9 and SaCas9 and top 5 peptides for AAV8 and AAVDJ were selected for synthesis by Synthetic Biomolecules as crude materials. For MHCI, we selected the top 20 peptides for SpCas9 and SaCas9 and the top 10 for AAV8 and AAVDJ. All of the peptides were dissolved in DMSO with a concentration of 40 mg  $ml^{-1}$  and stored at  $-20^\circ C$ .

**IFN $\gamma$  ELISPOT assay.** CD8<sup>+</sup> T cells were isolated from splenocytes using magnetic bead positive selection (Miltenyi Biotec) 6 weeks after virus infection. A total of  $2 \times 10^5$  CD8<sup>+</sup> T cells were stimulated with  $1 \times 10^5$  lipopolysaccharide blasts loaded with 10  $\mu$ g of individual peptide in 96-well flat-bottom plates (Immobilon-P, Millipore) that were coated with anti-IFN $\gamma$  monoclonal antibodies (clone AN18, Mabtech) in triplicate. Concanavalin A was used as positive control. After 20 h of incubation, biotinylated anti-mouse IFN $\gamma$  monoclonal antibodies (R4-6A2; Mabtech), followed by ABC peroxidase (Vector Laboratories) and then 3-amino-9-ethylcarbazole (Sigma-Aldrich) were added to the wells. Responses are expressed as number of IFN $\gamma$  spot-forming cells (SFC) per  $1 \times 10^6$  CD8<sup>+</sup> T cells.

**Reporting Summary.** Further information on research design is available in the Nature Research Reporting Summary linked to this article.

## Data availability

The authors declare that the main data supporting the results of this study are available within the paper and its Supplementary Information. The raw and analysed datasets generated during the study are available for research purposes from the corresponding author on reasonable request.

## Code availability

All code, input and output files used in this study are publicly available on GitHub (<https://github.com/natepalmer/immune-orthogonal>). Additional modified scripts can be accessed on request.

Received: 27 January 2018; Accepted: 16 June 2019;  
Published online: 22 July 2019

## References

- Mingozi, F. & High, K. A. Immune responses to AAV vectors: overcoming barriers to successful gene therapy. *Blood* **122**, 23–36 (2013).
- Zaldumbide, A. & Hoeber, R. C. How not to be seen: immune-evasion strategies in gene therapy. *Gene Ther.* **15**, 239–246 (2008).
- Yang, Y., Li, Q., Ertl, H. C. & Wilson, J. M. Cellular and humoral immune responses to viral antigens create barriers to lung-directed gene therapy with recombinant adenoviruses. *J. Virol.* **69**, 2004–2015 (1995).
- Jawa, V. et al. T-cell dependent immunogenicity of protein therapeutics: preclinical assessment and mitigation. *Clin. Immunol.* **149**, 534–555 (2013).
- Mays, L. E. & Wilson, J. M. The complex and evolving story of T cell activation to AAV vector-encoded transgene products. *Mol. Ther.* **19**, 16–27 (2011).
- Basner-Tschakarjan, E., Bijjiga, E. & Martino, A. T. Pre-clinical assessment of immune responses to adeno-associated virus (AAV) vectors. *Front. Immunol.* **5**, 28 (2014).
- Ertl, H. C. J. & High, K. A. Impact of AAV capsid-specific T-cell responses on design and outcome of clinical gene transfer trials with recombinant adeno-associated viral vectors: an evolving controversy. *Hum. Gene Ther.* **28**, 328–337 (2017).
- Kotterman, M. A., Chalberg, T. W. & Schaffer, D. V. Viral vectors for gene therapy: translational and clinical outlook. *Annu. Rev. Biomed. Eng.* **17**, 63–89 (2015).
- Mingozi, F. & High, K. A. Therapeutic in vivo gene transfer for genetic disease using AAV: progress and challenges. *Nat. Rev. Genet.* **12**, 341–355 (2011).
- Manno, C. S. et al. Successful transduction of liver in hemophilia by AAV-Factor IX and limitations imposed by the host immune response. *Nat. Med.* **12**, 342–347 (2006).
- Chew, W. L. Immunity to CRISPR Cas9 and Cas12a therapeutics. *Wiley Interdiscip. Rev. Syst. Biol. Med.* **10**, e1408 (2018).
- Sathish, J. G. et al. Challenges and approaches for the development of safer immunomodulatory biologics. *Nat. Rev. Drug Discov.* **12**, 306–324 (2013).
- Harding, F. A., Stickler, M. M., Razo, J. & DuBridge, R. B. The immunogenicity of humanized and fully human antibodies: residual immunogenicity resides in the CDR regions. *MAbs* **2**, 256–265 (2010).
- De Groot, A. S., Knopp, P. M. & Martin, W. De-immunization of therapeutic proteins by T-cell epitope modification. *Dev. Biol.* **122**, 171–194 (2005).
- Tangri, S. et al. Rationally engineered therapeutic proteins with reduced immunogenicity. *J. Immunol.* **174**, 3187–3196 (2005).
- Ferdosi, S. R. et al. Multifunctional CRISPR/Cas9 with engineered immunosilenced human T cell epitopes. *Nat. Commun.* **10**, 1842 (2019).
- Salvat, R. S., Choi, Y., Bishop, A., Bailey-Kellogg, C. & Griswold, K. E. Protein deimmunization via structure-based design enables efficient epitope deletion at high mutational loads. *Biotechnol. Bioeng.* **112**, 1306–1318 (2015).
- Armstrong, J. K. et al. Antibody against poly(ethylene glycol) adversely affects PEG-asparaginase therapy in acute lymphoblastic leukemia patients. *Cancer* **110**, 103–111 (2007).
- Ganson, N. J., Kelly, S. J., Scarlett, E., Sundry, J. S. & Hershfield, M. S. Control of hyperuricemia in subjects with refractory gout, and induction of antibody against poly(ethylene glycol) (PEG), in a phase I trial of subcutaneous PEGylated urate oxidase. *Arthritis Res. Ther.* **8**, R12 (2006).
- Veronese, F. M. & Mero, A. The impact of PEGylation on biological therapies. *BioDrugs* **22**, 315–329 (2008).
- Jevševar, S., Kunstelj, M. & Porekar, V. G. PEGylation of therapeutic proteins. *Biotechnol. J.* **5**, 113–128 (2010).
- Jacobs, F., Gordts, S. C., Muthuramu, I. & De Geest, B. The liver as a target organ for gene therapy: state of the art, challenges, and future perspectives. *Pharmaceuticals* **5**, 1372–1392 (2012).
- Kok, C. Y. et al. Adeno-associated virus-mediated rescue of neonatal lethality in argininosuccinate synthetase-deficient mice. *Mol. Ther.* **21**, 1823–1831 (2013).
- Courtenay-Luck, N. S., Epenetos, A. A. & Moore, R. Development of primary and secondary immune responses to mouse monoclonal antibodies used in the diagnosis and therapy of malignant neoplasms. *Cancer Res.* **46**, 6489–6493 (1986).
- Jinek, M. et al. A programmable dual-RNA-guided DNA endonuclease in adaptive bacterial immunity. *Science* **337**, 816–822 (2012).
- Mali, P. et al. RNA-guided human genome engineering via Cas9. *Science* **339**, 823–826 (2013).
- Moreno, A. M. & Mali, P. Therapeutic genome engineering via CRISPR-Cas systems. *Wiley Interdiscip. Rev. Syst. Biol. Med.* **9**, e1380 (2017).
- Gasiunas, G., Barrangou, R., Horvath, P. & Siksnys, V. Cas9-crRNA ribonucleoprotein complex mediates specific DNA cleavage for adaptive immunity in bacteria. *Proc. Natl Acad. Sci. USA* **109**, E2579–E2586 (2012).

29. Cong, L. et al. Multiplex genome engineering using CRISPR/Cas systems. *Science* **339**, 819–823 (2013).
30. Ran, F. A. et al. In vivo genome editing using *Staphylococcus aureus* Cas9. *Nature* **520**, 186–191 (2015).
31. Jinek, M. et al. RNA-programmed genome editing in human cells. *eLife* **2**, e00471 (2013).
32. Mali, P., Esvelt, K. M. & Church, G. M. Cas9 as a versatile tool for engineering biology. *Nat. Methods* **10**, 957–963 (2013).
33. Hsu, P. D., Lander, E. S. & Zhang, F. Development and applications of CRISPR-Cas9 for genome engineering. *Cell* **157**, 1262–1278 (2014).
34. Kelton, W. J., Pesch, T., Matile, S. & Reddy, S. T. Surveying the delivery methods of CRISPR/Cas9 for ex vivo mammalian cell engineering. *Chim. Int. J. Chem.* **70**, 439–442 (2016).
35. Cho, S. W., Kim, S., Kim, J. M. & Kim, J.-S. Targeted genome engineering in human cells with the Cas9 RNA-guided endonuclease. *Nat. Biotechnol.* **31**, 230–232 (2013).
36. Koonin, E. V., Makarova, K. S. & Zhang, F. Diversity, classification and evolution of CRISPR-Cas systems. *Curr. Opin. Microbiol.* **37**, 67–78 (2017).
37. Makarova, K. S. et al. An updated evolutionary classification of CRISPR-Cas systems. *Nat. Rev. Microbiol.* **13**, 722–736 (2015).
38. Chylinski, K., Makarova, K. S., Charpentier, E. & Koonin, E. V. Classification and evolution of type II CRISPR-Cas systems. *Nucleic Acids Res.* **42**, 6091–6105 (2014).
39. Shmakov, S. et al. Diversity and evolution of class 2 CRISPR-Cas systems. *Nat. Rev. Microbiol.* **15**, 169–182 (2017).
40. Crawley, A. B., Henriksen, J. R. & Barrangou, R. CRISPRdisco: an automated pipeline for the discovery and analysis of CRISPR-Cas systems. *CRISPR J.* **1**, 171–181 (2018).
41. Charlesworth, C. T. et al. Identification of pre-existing adaptive immunity to Cas9 proteins in humans. *Nat. Med.* **25**, 249–254 (2019).
42. Wagner, D. L. et al. High prevalence of *Streptococcus pyogenes* Cas9-reactive T cells within the adult human population. *Nat. Med.* **25**, 242–248 (2019).
43. Simhadri, V. L. et al. Prevalence of pre-existing antibodies to CRISPR-associated nuclease Cas9 in the US population. *Mol. Ther. Methods Clin. Dev.* **10**, 105–112 (2018).
44. Wagner, J. A. et al. Safety and biological efficacy of an adeno-associated virus vector-cystic fibrosis transmembrane regulator (AAV-CFTR) in the cystic fibrosis maxillary sinus. *Laryngoscope* **109**, 266–274 (1999).
45. Song, S. et al. Sustained secretion of human alpha-1-antitrypsin from murine muscle transduced with adeno-associated virus vectors. *Proc. Natl Acad. Sci. USA* **95**, 14384–14388 (1998).
46. Chirmule, N. et al. Humoral immunity to adeno-associated virus type 2 vectors following administration to murine and nonhuman primate muscle. *J. Virol.* **74**, 2420–2425 (2000).
47. Fields, P. A. et al. Risk and prevention of anti-factor IX formation in AAV-mediated gene transfer in the context of a large deletion of F9. *Mol. Ther.* **4**, 201–210 (2001).
48. Herzog, R. W. et al. Influence of vector dose on factor IX-specific T and B cell responses in muscle-directed gene therapy. *Hum. Gene Ther.* **13**, 1281–1291 (2002).
49. Lozier, J. N., Tayebi, N. & Zhang, P. Mapping of genes that control the antibody response to human factor IX in mice. *Blood* **105**, 1029–1035 (2005).
50. Zhang, H. G. et al. Genetic analysis of the antibody response to AAV2 and factor IX. *Mol. Ther.* **11**, 866–874 (2005).
51. Tam, H. H. et al. Sustained antigen availability during germinal center initiation enhances antibody responses to vaccination. *Proc. Natl Acad. Sci. USA* **113**, E6639–E6648 (2016).
52. Chew, W. L. et al. A multifunctional AAV-CRISPR-Cas9 and its host response. *Nat. Methods* **13**, 868–874 (2016).
53. Benveniste, O. et al. Prevalence of serum IgG and neutralizing factors against adeno-associated virus (AAV) types 1, 2, 5, 6, 8, and 9 in the healthy population: implications for gene therapy using AAV vectors. *Hum. Gene Ther.* **21**, 704–712 (2010).
54. Gao, G.-P. et al. Novel adeno-associated viruses from rhesus monkeys as vectors for human gene therapy. *Proc. Natl Acad. Sci. USA* **99**, 11854–11859 (2002).
55. Jooss, K., Yang, Y., Fisher, K. J. & Wilson, J. M. Transduction of dendritic cells by DNA viral vectors directs the immune response to transgene products in muscle fibers. *J. Virol.* **72**, 4212–4223 (1998).
56. Gernoux, G. et al. Early interaction of adeno-associated virus serotype 8 vector with the host immune system following intramuscular delivery results in weak but detectable lymphocyte and dendritic cell transduction. *Hum. Gene Ther.* **26**, 1–13 (2015).
57. Zhu, J., Huang, X. & Yang, Y. The TLR9-MyD88 pathway is critical for adaptive immune responses to adeno-associated virus gene therapy vectors in mice. *J. Clin. Invest.* **119**, 2388–2398 (2009).
58. Gernoux, G., Wilson, J. M. & Mueller, C. Regulatory and exhausted T cell responses to AAV capsid. *Hum. Gene Ther.* **28**, 338–349 (2017).
59. Kurosaki, T., Kometani, K. & Ise, W. Memory B cells. *Nat. Rev. Immunol.* **15**, 149–159 (2015).
60. Zabel, F. et al. Distinct T helper cell dependence of memory B-cell proliferation versus plasma cell differentiation. *Immunology* **150**, 329–342 (2017).
61. Ding, Q. et al. Permanent alteration of PCSK9 with in vivo CRISPR-Cas9 genome editing. *Circ. Res.* **115**, 488–492 (2014).
62. Zinn, E. et al. In silico reconstruction of the viral evolutionary lineage yields a potent gene therapy vector. *Cell Rep.* **12**, 1056–1068 (2017).
63. Calcedo, R. & Wilson, J. M. AAV natural infection induces broad cross-neutralizing antibody responses to multiple AAV serotypes in chimpanzees. *Hum. Gene Ther. Clin. Dev.* **27**, 79–82 (2016).
64. Harbison, C. E. et al. Examining the cross-reactivity and neutralization mechanisms of a panel of mAbs against adeno-associated virus serotypes 1 and 5. *J. Gen. Virol.* **93**, 347–355 (2012).
65. Majowicz, A. et al. Successful repeated hepatic gene delivery in mice and non-human primates achieved by sequential administration of AAV5<sup>ch</sup> and AAV1. *Mol. Ther.* **25**, 1831–1842 (2017).
66. McIntosh, J. H. et al. Successful attenuation of humoral immunity to viral capsid and transgenic protein following AAV-mediated gene transfer with a non-depleting CD4 antibody and cyclosporine. *Gene Ther.* **19**, 78–85 (2012).
67. Mingozzi, F. et al. Prevalence and pharmacological modulation of humoral immunity to AAV vectors in gene transfer to synovial tissue. *Gene Ther.* **20**, 417–424 (2013).
68. Mingozzi, F. et al. Pharmacological modulation of humoral immunity in a nonhuman primate model of AAV gene transfer for hemophilia B. *Mol. Ther.* **20**, 1410–1416 (2017).
69. Unzu, C. et al. Transient and intensive pharmacological immunosuppression fails to improve AAV-based liver gene transfer in non-human primates. *J. Transl. Med.* **10**, 122 (2012).
70. Riechmann, L., Clark, M., Waldmann, H. & Winter, G. Reshaping human antibodies for therapy. *Nature* **332**, 323–327 (1988).
71. Amabile, A. et al. Inheritable silencing of endogenous genes by hit-and-run targeted epigenetic editing. *Cell* **167**, 219–232 (2016).
72. Hinderer, C. et al. Severe toxicity in nonhuman primates and piglets following high-dose intravenous administration of an AAV vector expressing human SMN. *Hum. Gene Ther.* **29**, 285–298 (2018).
73. Vollmers, C., Sit, R. V., Weinstein, J. A., Dekker, C. L. & Quake, S. R. Genetic measurement of memory B-cell recall using antibody repertoire sequencing. *Proc. Natl Acad. Sci. USA* **110**, 13463–13468 (2013).
74. Adamopoulou, E. et al. Exploring the MHC-peptide matrix of central tolerance in the human thymus. *Nat. Commun.* **4**, 2039 (2013).
75. Ruppert, J. et al. Prominent role of secondary anchor residues in peptide binding to HLA-A2.1 molecules. *Cell* **74**, 929–937 (2017).
76. Zhang, S.-Q. et al. Direct measurement of T cell receptor affinity and sequence from naïve antiviral T cells. *Sci. Transl. Med.* **8**, 341ra77 (2016).
77. Baker, M. P., Reynolds, H. M., Lumicisi, B. & Bryson, C. J. Immunogenicity of protein therapeutics: the key causes, consequences and challenges. *Self Nonself* **1**, 314–322 (2010).
78. EL-Manzalawy, Y., Dobbs, D. & Honavar, V. Predicting linear B-cell epitopes using string kernels. *J. Mol. Recognit.* **21**, 243–255 (2008).
79. Larsen, J. E. P., Lund, O. & Nielsen, M. Improved method for predicting linear B-cell epitopes. *Immunome Res.* **2**, 2 (2006).
80. Sollner, J. et al. Analysis and prediction of protective continuous B-cell epitopes on pathogen proteins. *Immunome Res.* **4**, 1 (2008).
81. Dalkas, G. A. & Rومان, M. SEPIa, a knowledge-driven algorithm for predicting conformational B-cell epitopes from the amino acid sequence. *BMC Bioinform.* **18**, 95 (2017).
82. Sun, P. et al. Bioinformatics resources and tools for conformational B-cell epitope prediction. *Comput. Math. Methods Med.* **2013**, 943636 (2013).
83. Liepe, J. et al. A large fraction of HLA class I ligands are proteasome-generated spliced peptides. *Science* **354**, 354–358 (2016).
84. Fonfara, I. et al. Phylogeny of Cas9 determines functional exchangeability of dual-RNA and Cas9 among orthologous type II CRISPR-Cas systems. *Nucleic Acids Res.* **42**, 2577–2590 (2014).
85. Burstein, D. et al. New CRISPR-Cas systems from uncultivated microbes. *Nature* **542**, 237–241 (2016).
86. Shmakov, S. et al. Discovery and functional characterization of diverse class 2 CRISPR-Cas systems. *Mol. Cell* **60**, 385–397 (2015).
87. Andreatta, M. & Nielsen, M. Gapped sequence alignment using artificial neural networks: application to the MHC class I system. *Bioinformatics* **32**, 511–517 (2015).
88. Andreatta, M. et al. Accurate pan-specific prediction of peptide-MHC class II binding affinity with improved binding core identification. *Immunogenetics* **67**, 641–650 (2015).
89. Vita, R. et al. The immune epitope database (IEDB) 3.0. *Nucleic Acids Res.* **43**, D405–D412 (2015).
90. Truong, D.-J. J. et al. Development of an intein-mediated split-Cas9 system for gene therapy. *Nucleic Acids Res.* **43**, 6450–6458 (2015).

91. Moreno, A. M. et al. In situ gene therapy via AAV-CRISPR-Cas9-mediated targeted gene regulation. *Mol. Ther.* **26**, 1818–1827 (2018).
92. Grieger, J. C., Choi, V. W. & Samulski, R. J. Production and characterization of adeno-associated viral vectors. *Nat. Protoc.* **1**, 1412–1428 (2006).
93. Schubert, M., Lindgreen, S. & Orlando, L. AdapterRemoval v2: rapid adapter trimming, identification, and read merging. *BMC Res. Notes* **9**, 88 (2016).
94. Pinello, L. et al. Analyzing CRISPR genome-editing experiments with CRISPResso. *Nat. Biotechnol.* **34**, 695–697 (2016).
95. Clemente, T., Dominguez, M. R., Vieira, N. J., Rodrigues, M. M. & Amarante-Mendes, G. P. In vivo assessment of specific cytotoxic T lymphocyte killing. *Methods* **61**, 105–109 (2013).

### Acknowledgements

We thank members of the Mali laboratory for advice and help with experiments and the Salk GT3 viral core for help with the production of AAVs. This research was supported by UCSD Institutional Funds, the Burroughs Wellcome Fund (1013926), the March of Dimes Foundation (5-FY15-450), the Kimmel Foundation (SKF-16-150), and NIH grants (R01HG009285, RO1CA222826, RO1GM123313, R01AI079031 and R01AI106005). A.M.M. acknowledges a graduate fellowship from CONACYT and UCMEXUS. W.L.C. acknowledges the IAF-PP grant (H17/01/a0/012).

### Author contributions

A.M.M. designed and performed experiments, analysed the data and wrote the manuscript. N.P. performed the in silico analysis, designed and performed experiments,

analysed the data and wrote the manuscript. F.A. performed the ELISPOT experiments and analysed the data. G.C. and A.P. helped to perform experiments. N.J., W.L.C. and M.L. helped to design experiments. P.M. supervised the project, designed and helped to perform experiments and wrote the manuscript.

### Competing interests

A.M.M., N.P. and P.M. have filed patents on the basis of this research. P.M. is a scientific co-founder of Navega Therapeutics, Pretzel Therapeutics, Seven Therapeutics, Engine Biosciences and Shape Therapeutics. The terms of these arrangements have been reviewed and approved by the University of California, San Diego in accordance with its policies regarding conflicts of interest. W.L.C. is a scientific co-founder of Seven Therapeutics. N.J. is a scientific advisor of ImmDX, LLC and Immune Arch, Inc.

### Additional information

**Supplementary information** is available for this paper at <https://doi.org/10.1038/s41551-019-0431-2>.

**Reprints and permissions information** is available at [www.nature.com/reprints](http://www.nature.com/reprints).

**Correspondence and requests for materials** should be addressed to P.M.

**Publisher's note:** Springer Nature remains neutral with regard to jurisdictional claims in published maps and institutional affiliations.

© The Author(s), under exclusive licence to Springer Nature Limited 2019

## Reporting Summary

Nature Research wishes to improve the reproducibility of the work that we publish. This form provides structure for consistency and transparency in reporting. For further information on Nature Research policies, see [Authors & Referees](#) and the [Editorial Policy Checklist](#).

### Statistics

For all statistical analyses, confirm that the following items are present in the figure legend, table legend, main text, or Methods section.

- |     |           |
|-----|-----------|
| n/a | Confirmed |
|-----|-----------|
- The exact sample size ( $n$ ) for each experimental group/condition, given as a discrete number and unit of measurement
  - A statement on whether measurements were taken from distinct samples or whether the same sample was measured repeatedly
  - The statistical test(s) used AND whether they are one- or two-sided  
*Only common tests should be described solely by name; describe more complex techniques in the Methods section.*
  - A description of all covariates tested
  - A description of any assumptions or corrections, such as tests of normality and adjustment for multiple comparisons
  - A full description of the statistical parameters including central tendency (e.g. means) or other basic estimates (e.g. regression coefficient) AND variation (e.g. standard deviation) or associated estimates of uncertainty (e.g. confidence intervals)
  - For null hypothesis testing, the test statistic (e.g.  $F$ ,  $t$ ,  $r$ ) with confidence intervals, effect sizes, degrees of freedom and  $P$  value noted  
*Give  $P$  values as exact values whenever suitable.*
  - For Bayesian analysis, information on the choice of priors and Markov chain Monte Carlo settings
  - For hierarchical and complex designs, identification of the appropriate level for tests and full reporting of outcomes
  - Estimates of effect sizes (e.g. Cohen's  $d$ , Pearson's  $r$ ), indicating how they were calculated

*Our web collection on [statistics for biologists](#) contains articles on many of the points above.*

### Software and code

Policy information about [availability of computer code](#)

Data collection

netMHC software used to predict peptide binding to MHC molecules is cited in the primary literature and available online.

Data analysis

Custom scripts used for k-mer analysis, compiling netMHC output, and assembling immune orthogonal cliques are publicly available on GitHub at <https://github.com/natepalmer/immune-orthogonal>

For manuscripts utilizing custom algorithms or software that are central to the research but not yet described in published literature, software must be made available to editors/reviewers. We strongly encourage code deposition in a community repository (e.g. GitHub). See the Nature Research [guidelines for submitting code & software](#) for further information.

### Data

Policy information about [availability of data](#)

All manuscripts must include a [data availability statement](#). This statement should provide the following information, where applicable:

- Accession codes, unique identifiers, or web links for publicly available datasets
- A list of figures that have associated raw data
- A description of any restrictions on data availability

The authors declare that the main data supporting the results in this study are available within the paper and its Supplementary Information. The raw and analysed datasets generated during the study are available for research purposes from the corresponding authors on reasonable request.

## Field-specific reporting

Please select the one below that is the best fit for your research. If you are not sure, read the appropriate sections before making your selection.

Life sciences  Behavioural & social sciences  Ecological, evolutionary & environmental sciences

For a reference copy of the document with all sections, see [nature.com/documents/nr-reporting-summary-flat.pdf](https://www.nature.com/documents/nr-reporting-summary-flat.pdf)

## Life sciences study design

All studies must disclose on these points even when the disclosure is negative.

Sample size	We initially hypothesized that antibody production may vary greatly from mouse-to-mouse, and so to capture this variability we began by choosing n=6 per experimental group, and n=6 per control group. Correspondingly when using AAV-8-SaCas9 targeting a gene (PCSK9) (n=6), we also had n=6 for our non-targeted control (empty). We also ran a pilot study that received AAV-8-SaCas9 (n=12 total), and we confirmed that antibodies were indeed being robustly generated against both the AAV-8 Capsid and the SaCas9, and based on this we expanded our study to include additional capsids (AAV-8, AAV-DJ, AAV-2, AAV-5) and two different Cas9 proteins (SaCas9 and SpCas9). Thereafter we continued with n=6 or higher per experimental group.
Data exclusions	Mouse #4 injected with AAV2 and AAV5 were excluded because these mice died at the week 6 time point. We thus didn't include any data for this mouse, even though we had data for weeks 0–5.
Replication	We first ran a pilot experiment to determine antibody production against AAV-8 and SaCas9 targeting PCSK9 or an empty control (Fig. 1 d,e). After confirming antibody production, we ran more extensive experiments as follows: AAV8-SaCas9, AAV8-SpCas9, AAVDJ-SaCas9, and AAVDJ-SpCas9. These constructs targeted the apoB gene (n=6) and a non-targeting control (n=6). In addition, we also immunized mice with AAV-2-mCherry and AAV-5-mCherry (n=6 each), to expand our AAV repertoire. We were thereby able to reproduce the immune responses to SpCas9 and SaCas9, and AAV-8 and AAV-DJ via these separate studies. We also performed two distinct immunization methods (one via AAV-SpCas9 or SaCas9 and another via CFA-SpCas9 or SaCas9) to replicate our multi-dosing experiment.
Randomization	All mice were bled at the baseline time point and were then randomly assigned into an experimental group.
Blinding	One researcher collected serum from mice and a different researcher conducted the ELISAs and ELISA analysis, and was thus blinded from group allocation.

## Reporting for specific materials, systems and methods

We require information from authors about some types of materials, experimental systems and methods used in many studies. Here, indicate whether each material, system or method listed is relevant to your study. If you are not sure if a list item applies to your research, read the appropriate section before selecting a response.

### Materials & experimental systems

n/a	Involvement in the study
<input type="checkbox"/>	<input checked="" type="checkbox"/> Antibodies
<input type="checkbox"/>	<input checked="" type="checkbox"/> Eukaryotic cell lines
<input checked="" type="checkbox"/>	<input type="checkbox"/> Palaeontology
<input type="checkbox"/>	<input checked="" type="checkbox"/> Animals and other organisms
<input checked="" type="checkbox"/>	<input type="checkbox"/> Human research participants
<input checked="" type="checkbox"/>	<input type="checkbox"/> Clinical data

### Methods

n/a	Involvement in the study
<input checked="" type="checkbox"/>	<input type="checkbox"/> ChIP-seq
<input type="checkbox"/>	<input checked="" type="checkbox"/> Flow cytometry
<input checked="" type="checkbox"/>	<input type="checkbox"/> MRI-based neuroimaging

## Antibodies

Antibodies used	<ol style="list-style-type: none"> <li>1. PCSK9 Capture antibody. Vendor: R&amp;D systems, Cat. #: MPC900, Lot: 339259</li> <li>2. HRP-labeled goat anti-mouse IgG1. Vendor: Bethyl, Cat. #: A90-131P</li> <li>3. IFN-<math>\gamma</math> mAb R4-6A2. Vendor: Mabtech, Cat. #: 3321-6-250, Batch:11</li> <li>4. anti-IFN-<math>\gamma</math> mAb clone AN18. Vendor: Mabtech, Cat# 3321-3-1000, batch 12</li> </ol>
Validation	<p>All antibodies were validated based on previous publications as follows:</p> <ol style="list-style-type: none"> <li>1. PCSK9 Capture antibody. Publication: Dong B. et al., J Biol Chem, 2015;290(7):4047-58.</li> <li>2. HRP-labeled goat anti-mouse IgG1. Publication: Pfeifle R. et al, Nature Immunology, 2017;18(1): 104-113.</li> <li>3. IFN-<math>\gamma</math> mAb R4-6A2. Publication: Lindestam Arlehamn C.S. et al., Proc Natl Acad Sci U S A. 2015;112(2):E147-55.</li> <li>4. anti-IFN-<math>\gamma</math> mAb clone AN18. Publication: Bourgeois-Daigneault MC et al., Sci Transl Med., 2018;10(422).</li> </ol>

## Eukaryotic cell lines

Policy information about [cell lines](#)

Cell line source(s)	HEK293T cells were utilized for AAV production
Authentication	Cells were acquired from ATCC: 293 [HEK-293]ATCC® CRL-1573™ and were not validated post-acquisition.
Mycoplasma contamination	Cell lines were tested by the vendor for mycoplasma contamination prior to acquisition.
Commonly misidentified lines (See <a href="#">ICLAC</a> register)	No commonly misidentified cell lines were used.

## Animals and other organisms

Policy information about [studies involving animals](#); [ARRIVE guidelines](#) recommended for reporting animal research

Laboratory animals	10 week-old adult male C57BL/6J or BALB/c mice.
Wild animals	The study did not involve wild animals.
Field-collected samples	The study did not involve samples collected from the field.
Ethics oversight	All animal procedures were performed in accordance with protocols approved by the Institutional Animal Care and Use Committee (IACUC) of the University of California, San Diego.

Note that full information on the approval of the study protocol must also be provided in the manuscript.

## Flow Cytometry

### Plots

Confirm that:

- The axis labels state the marker and fluorochrome used (e.g. CD4-FITC).
- The axis scales are clearly visible. Include numbers along axes only for bottom left plot of group (a 'group' is an analysis of identical markers).
- All plots are contour plots with outliers or pseudocolor plots.
- A numerical value for number of cells or percentage (with statistics) is provided.

### Methodology

Sample preparation	Briefly, spleens from adult C57BL/6J mice were harvested and treated to remove erythrocytes and dead cells. These cells were then diluted to 10E+7 cells/ml and split into two pools, one of which was pulsed for 40 min with a pool of the 30 most immunogenic T-cell epitopes in SpCas9 (according to our predictions) at 1 µg/ml each and labeled with the CellTrace Violet fluorescent dye (ThermoFisher). The other pool was pulsed with a matching amount of DMSO, and labeled with the green fluorescent dye CFSE (ThermoFisher). A 1:1 mixture of these cells were then injected into naïve or CFA-immunized mice at week 1 or 3.5 retro-orbitally at 3-6 x 10E+7 cells per mouse. Spleens from these mice were harvested 16-20 hours later, treated to remove erythrocytes, and analyzed by flow cytometry to assess the degree of specific clearance of the CTV+ cells which were pulsed with Cas9 peptides.
Instrument	BD FACSAria Fusion
Software	BD FACSDiva 8.0.1 Global
Cell population abundance	Pulsed and unpulsed splenocytes were injected at equal ratios. Pulsed and unpulsed splenocytes were between 0.9–1.2% of the total cell population, except for mice injected with SpCas9 pulsed splenocytes, which had around 0.3–0.5% of pulsed splenocytes due to T-cell clearance.
Gating strategy	Same gating was used for all flow-cytometry analyses.

Tick this box to confirm that a figure exemplifying the gating strategy is provided in the Supplementary Information.